ISSN1027-5495. Functional Materials, 30, No.4 (2023), p. 506-510
doi:http://dx.doi.org/10.15407/fm30.04.506

A new Mn(II) complex constructed from 4-[(8-hydroxy-5-quinolinyl)azo]-benzenesulfonic acid: synthesis, crystal structure and antibacterial property

Xuyao Zhu[1], Hongxu Bai[2], Liying Yu[2], Shijie Dong[1], Jiayue Liu[1], Huiying Wang[1], Yanan Luo[1]

[1] College of Pharmacy, Jilin Medical University, 5 Jilin Str., 132013, Jilin, P. R. China
[2] College of Chemical and Pharmaceutical Engineering, Jilin Institute of Chemical Technology, 45 Chengde Str., 132022, Jilin, P. R. China

Received October 22, 2023

By using 4-[(8-Hydroxy-5-quinolinyl)azo]-benzenesulfonic acid (H_2L) ligand, a new inorganic-organic hybrids formulated as $[Mn_{0.5}(L)(H_2O)]$ (**1**), has been synthesized successfully under conventional hydrothermal conditions. Complex **1** exhibits a zero-dimensional (0D) structure. In addition, the antibacterial property of complex **1** was tested. The antibacterial property of Gram-positive bacteria is slightly better than that of Gram-negative bacteria in complex **1**.

Keywords: 4-[(8-Hydroxy-5-quinolinyl)azo]-benzenesulfonic acid; hydrothermal synthesis; antibacterial property; azo coordination polymer

Новий комплекс Mn(II), побудований з 4-[(8-гідрокси-5-хінолініл)азо]-бензолсульфонової кислоти: синтез, кристалічна структура та антибактеріальні властивості. *Xuyao Zhu, Hongxu Bai, Liying Yu, Shijie Dong, Jiayue Liu, Huiying Wang, Yanan Luo*

Використовуючи ліганд 4-[(8-гідрокси-5-хінолініл)азо]бензолсульфонової кислоти (H_2L), було отримано нові неорганічні та органічні гібриди, сформульовані як $[Mn_{0.5}(L)(H_2O)]$ (1), що успішно синтезується в звичайних гідротермальних умовах. Комплекс **1** демонструє нуль-вимірну (0D) структуру. Крім того, була перевірена антибактеріальна властивість комплексу **1**. Антибактеріальні властивості грампозитивних бактерій виявилися трохи кращі, ніж у грамнегативних бактерій комплексу **1**.

1 Introduction

Multifunctional materials, such as azo coordination polymers, are attracting more and more significant research attention [1-3] due to their intriguing structures, excellent and extensive potential applications in catalysis, optics, separation, antibacterial properties and so on [4-7]. By exploiting the strategy of synergistic interaction of inorganic components and organic components, many examples of azo coordination polymers have been successfully synthesized under hydrothermal condition [8]. Currently, azo-compounds as rigid ligands have attracted much attention due to their versatile structure, high reactivity and abundant functionality [9]. The 8-Hydroxy-5-quinolinyl groups of azo-compounds, which exhibit good coordination abilities and diverse coordination modes in its oxygen/nitrogen donor atoms, are good candidates for useful organic linkers for joining azo coordination polymers [10]. Azo coordination polymers are mainly zero-dimen-

Table 1 Crystal data collections and structure refinements for complex **1**.

Complex **1**			
Formula	$C_{15}H_{11}Mn_{0.5}N_3O_5S$	Space group	I2/c
Fw	372.80	Temperature (K)	293(2)
Crystal system	monoclinic	*V* (nm)^3	3.0938(3)
a (nm)	1.5705 (10)	α (°)	90
b (nm)	0.8727(4)	*β* (°)	107.735(6)
c (nm)	2.3698(13)	γ (°)	90
Z	8	ρ_{calc} (g/m^3)	1.601
F(000)	1524.0	*μ* (mm^{-1})	0.632
θ range (°)	6.02-50.696	Reflections collected	5901
Independent reflections (R_{int})	2829(0.0522)	GOF	1.000
Final $R^{a,b}$ indices [$I>2\sigma(I)$]	$R_1 = 0.0625$ $wR_2 = 0.1169$	*R* indices (all data)	$R_1 = 0.1280$ $wR_2 = 0.1478$

$^*R_1 = \sum ||F_o| - |F_c|| / \sum |F|$. $^b wR_2 = |\sum w(|F_o|^2 - |F_c|^2)^2 / \sum |w(F)^2|^{1/2}$

sional (0D) and one-dimensional (1D) chain structures determined by the structure of the ligands, compared to many coordination polymers [11].

In this paper, the complex $[Mn_{0.5}(L)(H_2O)]$ (**1**) was successfully synthesized with 4-[(8-hydroxy-5-quinoline) azo]-benzenesulfonic acid. Complex **1** was characterized by X-ray diffraction analysis of single crystals, elemental analysis, thermogravimetric analysis and powder X-ray diffraction. Finally, the antibacterial property of complex **1** was investigated by using the bacteriostatic method and the growth curve method.

2. Experimental

Synthesis of ligand H_2L. 4-[(8-hydroxy-5-quinolinyl) azo]-benzenesulfonic acid was prepared according to the literature method [12].

Synthesis of $[Mn_{0.5}(L)(H_2O)]$ *(1).* Complex **1** was successfully synthesized by $MnCl_2$ and H_2L under conventional hydrothermal conditions. A mixture of H_2L (5 mg, 0.015 mmol), $MnCl_2$ (30 mg, 0.22 mmol), H_2O (2 mL) absolute ethyl alcohol (10 mL) and ethylenediamine (0.01 mL) was dissolved at room temperature for 1 h until a clear red solution formed. The mixture was kept stirring for 1 h at room temperature, finally put into a Teflon-lined autoclave and kept under autogenous pressure at 130 °C for 72 h. After slow cooling to room temperature, red rod crystals were filtered and washed with absolute ethyl alcohol and dried. For $C_{15}H_{11}Mn_{0.5}N_3O_5S$,

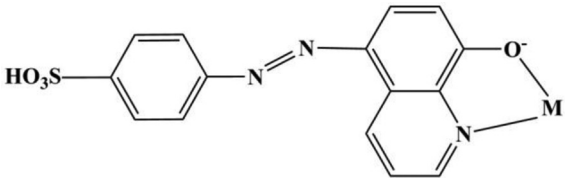

Scheme 1 The coordination mode of L^{2-} ligand.

(Mr = 372.80): C 48.33; H 2.97; N 11.27; found: C 48.37; H 2.92; N 11.31.

Structure determination. PXRD patterns were recorded on a Siemens D5005 diffractometer by using Cu-*K*α radiation (*λ* = 1.5418 Å) with a graphite monochromator. Elemental analyses for C, H and N were performed on a Perkin-Elmer 2400 Elemental Analyzer. IR (KBr pellets) spectra were recorded in the 4004000 cm^{-1} region on an Alpha Centaurt FT/IR spectrometer. The thermal behavior was studied by thermogravimetric analyses (TGA) on a Perkin-Elmer TGA 7 thermogravimetric analyzer under N_2 with a heating rate of 10 °C min^{-1}.

Complex **1** was stable under ambient conditions and single crystals were glued on thin glass fibers. Diffraction intensities were recorded on a Bruker Apex II CCD area-detector diffractometer (Mo-*Kα* 0.071073 nm). An empirical absorption correction was applied to the date using the SADABS program. The structure was identified by the direct method (SHELXS-97) and refined by full matrix least squares [13]. All non-hydrogen atoms were refined anisotropically. All hydrogen atoms were located geometrically by the program OLEX-2

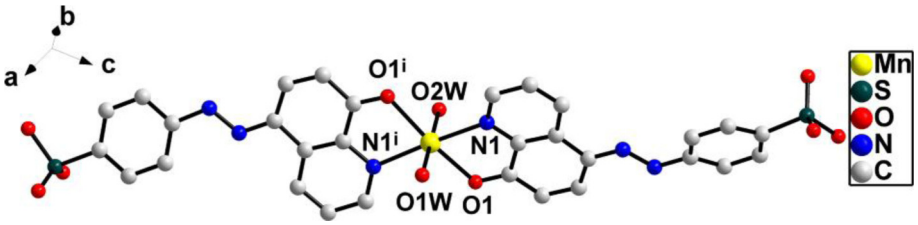

Fig. 1 The coordination environments of Mn1 in complex **1** (symmetry code: i, 1-x, y, 0.5-z . All hydrogen atoms are omitted for clarity).

[14]. The final formula was derived from crystallographic data combined with elemental and thermogravimetric analyses data. CCDC-2163958 contains the supplementary crystallographic data for this paper. Data collection and structure refinement details are summarized in Table 1.

Testing of Antibacterial property. Solution preparation for antibacterial experiment: The organic ligand (H_2L) solution with the concentration of 5 mg/mL was prepared by ultrasonic stirring of 50 mg organic ligand in 10 mL distilled water. About 50 mg of complex **1** was stirred in 5 mL of distilled water by ultrasonically agitation to prepare a complex **1** solution with a concentration of 10 mg/mL (Solution 1). 2.5 mL of the solution 1 was taken into 2.5 mL distilled water and ultrasonically stirred into a complex solution of 5 mg/mL (solution 2). Then 1.5 mL of the solution 2 was taken into 1.5 mL distilled water and ultrasonically stirred into a complex solution of 2.5 mg/mL (solution 3). Filter paper treatment: Filter paper sheets with a diameter of about 6 mm were placed into sterile distilled water, solution 1, solution 2 and solution 3 respectively for ultrasound treatment. After soaking for 1 h, they were taken out and placed in a clean Petri dish. Then they were placed on the aseptic operating table and irradiated with an ultraviolet lamp for sterilization. The disc diffusion method was used to determine the inhibition zones in the growth of bacterial species. Escherichia coli (ATCC25922) and Staphylococcus aureus (ATCC6538) were selected and inoculated into sterile nutrient agar. After the nutrient agar medium was cooled and shaped, filter papers of the blank water sample, solution 1, solution 2 and solution 3 were placed in a fixed position. Cultivation was carried out in an incubator with a constant temperature of 37° for 2-3 days and observed every 6 h.

Gram growth curve experiment: Complex **1** of different weights was dissolved in the sterilized liquid medium, sealed and stirred by ultrasound. Medium solutions containing complex **1** at concentrations of 0, 6.5, 12.5, 25, 50, 100, 200 and 400 μg/mL were placed in a sterile platform for UV irradiation for sterilization. A certain amount of Staphylococcus aureus culture was inoculated into the liquid medium with the same volume and different concentrations of complex **1**, and placed in an incubator of 37° for shock cultivation. At 0, 3, 6, 9, 12, 16, 18, 21 and 24 h, the absorbance of the above solution (including the same volume of Staphylococcus aureus and different concentrations of complex **1**) at fixed wavelength of 600 nm (according to the literature) was measured by an UV-Vis spectrophotometer [15].

3. Results and discussion

Single-crystal X-ray analysis shows that complex **1** crystallizes in monoclinic crystal system, I*2/c* space group, which exhibits a 0D coordination structure. The asymmetric unit of complex **1** consists of one half Mn(II) ion, one L^{2-} ligand and one coordinated water molecule. Mn1 is coordinated by two nitrogen atoms (N1 and $N1^i$) and two oxygen atoms (O1 and $O1^i$) from the quinolinol groups of two separated L^{2-} ligands, and two coordinated water molecules (O1W and O2W), exhibiting a distorted octahedral geometry (as shown in Fig. 1). In complex **1**, the quinoline group (O1 and N1) of each L^{2-} ligand adopts a bidentate chelating mode to coordinate one Mn(II) cation (Scheme 1). The Mn-O/N bond distances are in the range of [2.141(4)–2.231(4) Å], which are in the normal range of those observed in reported Mn(II) complexes [16].

The IR spectrum of complex **1** is given in Fig. 2, which shows the characteristic absorption peaks of H_2L. IR data (KBr pellet, cm^{-1}): 3257.5(w), 1750.6(w), 1700.4(w), 1650.8(m), 1625.9(s), 1568.5(s), 1540.2(w), 1520.5(m), 1490.2(s), 1380.8(s), 1372.2(m), 1254.3(w), 1204.7(s), 1198.5(w), 1140.4(m), 1125.5(w), 1064.3(m), 1007.6(w), 958.4(s), 900.7(s), 762.5(s), 745.8(s), 670.4(s), 648.3(w), 589.6(w).

In order to confirm the structural homogeneity of the bulk power materials, power X-ray

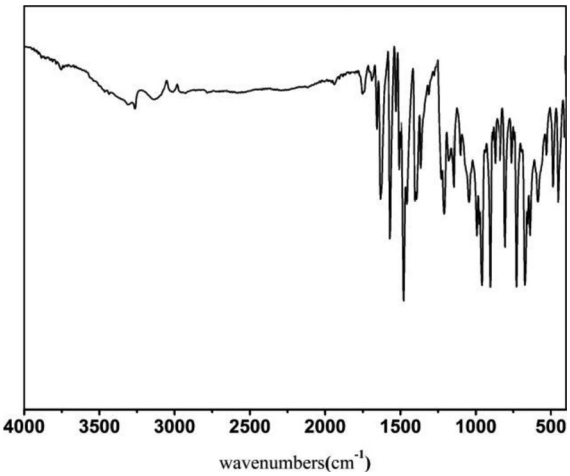

Fig. 2 IR curve of complex **1**.

diffraction (PXRD) experiment has been carried out. The PXRD experimental and computer simulated patterns are in good agreement with each other (Fig. 3), indicating phase purity of complex **1**.

The thermogravimetric analysis was performed for complex **1** in order to study thermal behavior more fully. The experiment was carried out under N_2 with a heating rate of 10 °C min^{-1}. As shown in Fig. 4, the TG curve of complex **1** shows the first weight loss of 4.86% occurring from 242 °C to 285 °C, corresponding to the release of one coordinated water molecule (calcd 4.83%). The second weight loss of 74.98% from 326 °C to 558 °C is due to the decomposition of L^{2-} ligand (calcd 74.92%).

As shown in Fig. 5, the antibacterial activities of complex **1** were studied against Gram-positive S. aureus and Gram-negative E. coli. The results showed that the low concentration had slightly antibacterial activity, but the medium concentration and high concentration of complex **1** had clear antibacterial activity against S. aureus. At the same concentration, the antimicrobial activity in Gram-negative bacteria was weaker than that in Gram-positive bacteria. The results indicated that complex **1** had a good antibacterial activity, which was mainly due to the synergistic effect of Mn^{2+} and H_2L ligands.

In order to further study and verify the antibacterial activities, the effect of complex **1** on the growth of S. aureus was tested. The results showed that the growth curve of S. aureus treated with 6.5, 12.5, 25 50 and 100 μg/mL complex **1** was almost the same as that treated with 0 μg/mL complex **1**, showing typical growth curve (Fig. 6). Therefore, it was

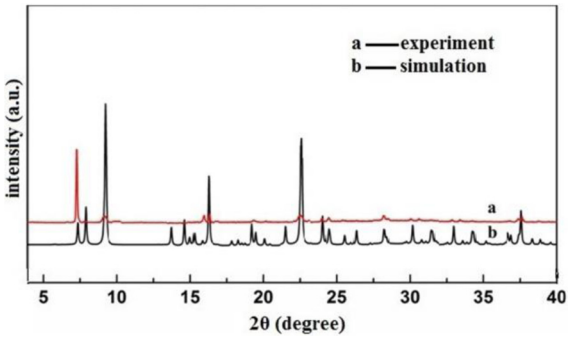

Fig. 3 The experimental (a) and simulative (b) powder X-ray diffraction patterns for complex **1**.

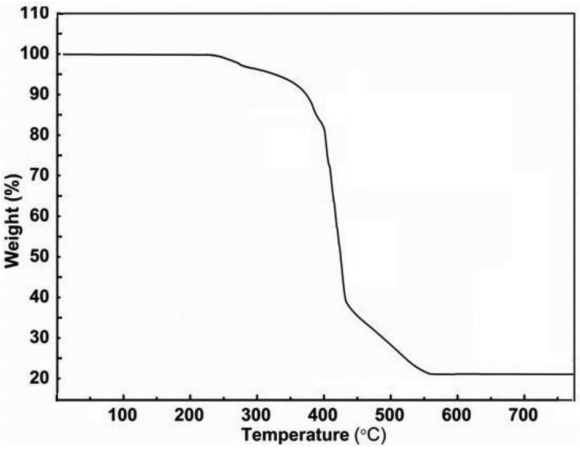

Fig. 4 TGA curve of complex 1.

shown that complex **1** had no inhibitory effect on S. aureus at low mass concentration. OD_{600} of S. aureus treated with 200 μg/mL of complex **1** showed no obvious change at about 0-9 h compared with OD_{600} of 0 μg/mL complex **1**. However, with the extension of time, the growth trend of S. aureus treated with 200 μg/mL complex **1** was slightly different from the control group and showed some antibacterial effect. OD_{600} treated with 400 μg/mL complex **1** showed significant antibacterial effect at about 0-9 h, and has since demonstrated antibacterial properties. Only complex **1** with mass concentrations more than 200 μg/mL could completely inhibit the proliferation and growth of S. aureus in the culture medium within 24 h. Complex **1** is an insoluble solid material, which may be a good solid antibacterial agent.

4. Conclusion

In summary, a new 0D Mn(II)-based coordination polymer, $[Mn_{0.5}(L)(H_2O)]$, has been self-assembled and synthesized under conventional hydrothermal conditions. Complex **1** showed good antibacterial properties in the inhibitory

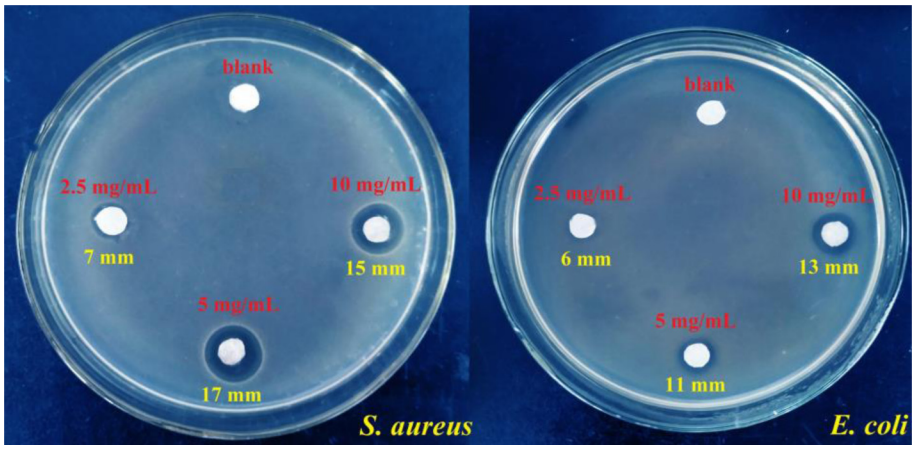

Fig.5 Optical photograph of complex **1** for positive S. aureus and negative E. coli.

region of Gram-positive S. aureus. And complex **1** with mass concentrations of more than 200 μg/mL could completely inhibit the proliferation and growth of S. aureus in the culture medium within 24 h. It also indicated that the crystal material of the complex **1** had a good application potential in the field of biology.

Acknowledgments

This work was supported by Innovation and Entrepreneurship Training Program of Jilin Medical University (Project Name: Design and synthesis of azo metal complexes and antibacterial and antitumor properties № 202313706013)

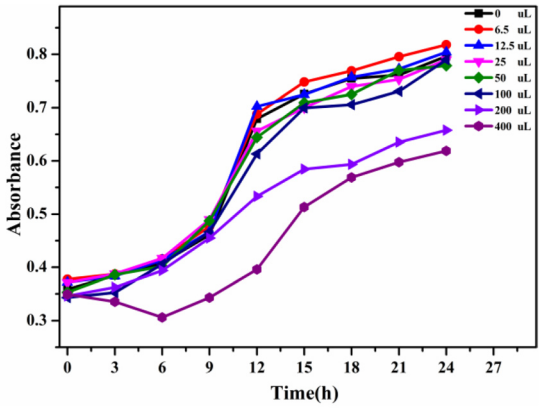

Fig. 6 Growth curves of E.coli in different concentrations of complex **1**

References

1. Y.P. Li, L.J. Zhang, W.J. Ji, *J. Mol. Struc.*, **1133**, 607 (2017).
2. J. Yan, L. Wilbraham, P.N. Basa, et al., *Inorg. Chem.*, **57**, 15009 (2018).
3. K. Stephen, U.T. Ashapak, M. Varnitha, et al., *J. Macromol. Sci.*, **60**, 580 (2023).
4. F. Sabahat, M.A. Naeem, I.H. Ul, et al., *J. Trace. Elem. Med. Bio.*, **80**, 127292 (2023).
5. C. Zhu, Q. Mao, D. Li, et al., *Catal. Commun.*, **104**, 123 (2018).
6. S. Taleghani, M. Mirzaei, H. E-Hosseini, et al., *Coord. Chem. Rev.*, **309**, 84(2016).
7. H. Sartzi, H.N. Miras, L. Vilà-Nadal, et al., *Angew. Chem. Int. Ed.*, **54**, 15488 (2015).
8. Y.N. Luo, X.Z. Xu, F.X. Sun, et al., *Chem. Res. Chin. Univ.*, **30**, 27 (2014).
9. F. Sabahat, A.M. Naeem, W. Muhammad, et al., *Inorg. Chem. Commun.*, **154**, (2023).
10. A.J. Lan, M. Padmanabhan, K.H. Li, et al., *Inorg. Chim. Acta.*, **366**, 68 (2011).
11. L.L. Zhang, C.Y. Lu, S.P. Chen, et al., *Inorg. Chem. Commun.*, **14**, 143 (2011).
12. J.S. Park, S. Jeong, S. Dho, et al., *Dyes Pigments*, **87**, 4954 (2010).
13. O.V. Dolomanov, L.J. Bourhis, R.J. Gildea, et al., *J. Appl. Crystallogr.*, **42**, 339 (2009).
14. G.M. Sheldrick. SHELXTL NT Crystal Structure Analysis Package[CP]. Version 5.10; Bruker AXS, Analytical X-ray System: Madison, WI, 1999.
15. H. Huang, W. Gao, F. Liu, et al., *Inorg. Chim. Acta.*, **484**, 414 (2019).
16. X.J. Duan, X.D. Du, B.B. Zhang, et al., *J. Med. Biol. Eng.*, **19**, 237 (2015).